

Use Of Mining Waste For The Production Of Coarse Aggregate For Concrete Manufacturing

Robson Da Silva Fernandes¹, João Carlos Lisboa De Lima¹,
Sabino Alves De Aguiar Neto², Rodrigo Rodrigues Da Cunha³,
Kleber Roberto Matos Da Silva³, Celestina Lima De Rezende Farias³,
Marcelo Martins Farias³, Elsimar Souza Santos¹,
Crislayne De Miranda Moraes¹, Elielson Oliveira De Sousa¹,
Leonardo Sousa Duarte⁴, Adonay Saráty De Carvalho¹,
Aldemar Batista Tavares De Sousa¹, Marcelo De Souza Picanço¹,
Alcebíades Negrão Macedo¹

¹ (Institute Of Technology, Faculty Of Civil Engineering / Federal University Of Pará, Brazil)

²(Civil Engineering / State University Of Pará)

³(Civil Engineering / Federal Institute Of Education, Science, And Technology Of Pará, Brazil)

⁴(Civil Engineering / University Of Amazônia, Brazil)

Abstract:

Background: The bauxite residue, also known as red mud, is a byproduct of the bauxite beneficiation process through the Bayer method, generated in large volumes and with significant environmental challenges. To minimize its impacts, this study proposes the production of synthetic coarse aggregates (SCA) from this residue, aiming for its application in Portland cement structural concrete.

Materials and Methods: The production process involved a preliminary step and three optimization cycles, with tests for evaluating chemical composition, bulk density, granulometry, shape index, water absorption, mechanical strength, and durability.

Results: In the third cycle, the aggregates achieved satisfactory geometric conformation, adequate strength, and good durability, although water absorption still needs to be reduced.

Conclusion: The results demonstrate the potential of this material as a sustainable alternative for the substitution of natural aggregates, contributing to the reduction of environmental impacts from mining.

Key Word: Synthetic coarse aggregate; bauxite residue; production cycles, tests.

Date of Submission: 08-02-2025

Date of Acceptance: 18-02-2025

I. Introduction

The exploitation of natural resources causes a shortage of raw materials, which drives the search for alternative materials, clean sustainability, and waste recycling techniques¹. In this way, there is a need to seek viable and economical alternative solutions in the construction industry as a means of overcoming the limitations of natural resources and reusing waste that is harmful to the environment².

The Brazilian Amazon has one of the largest and most diverse mineral reserves on the planet, and the state of Pará is the leading mining state in the Amazon, where the mineral sector accounts for 40% of exports and 12% of the state's Gross Domestic Product³.

The mineral extraction industry occupies a significant position as one of the most vital industries in the region, generating substantial economic and social effects on a national scale. However, its environmental effects lead to a negative impact in the areas where mining is carried out⁴.

Bauxite residue belongs to a group of waste materials known as "tailings," which result from the beneficiation of ores by the mineral extraction industry. These residues are soils that once contained the mineral of interest or result from the grinding of rocks. Depending on the extraction process, chemical substances may be added, such as caustic soda, which is used in alumina refining^{5,6}.

One of the biggest challenges faced by the bauxite beneficiation industry is the environmentally appropriate disposal of the waste generated during the clarification process, known as bauxite residue. This waste requires large areas for storage, and treating these areas (deposition ponds) is very costly^{7,8}. The construction of a storage basin requires an investment of approximately \$8.3 million⁹.

There are 85 alumina production plants worldwide, with an average bauxite residue generation of approximately 1.2 tons of sludge per ton of alumina produced. Annually, 169 million tons of this residue are generated worldwide, with around 2.5 billion tons currently stored^{10,11}.

For this reason, this field of study has gained momentum globally over the past decades, as both the public sector and private companies express enthusiasm for the discoveries made in this area. Waste recycling is a crucial and indispensable measure to mitigate the ecological impacts caused by large industrial manufacturing processes^{12,13}.

It has been proven that bauxite residue has great potential as a raw material when combined with silica and clay mixtures to produce synthetic coarse aggregates. This idea emerged from the increasing need to reduce, and eventually eliminate, the use of natural coarse aggregates in concrete applications. It presents an interesting alternative to decreasing the exploitation and use of natural aggregates.

In general, this research aligns with studies from various authors who confirm the technical feasibility of using bauxite residue to manufacture coarse aggregates, particularly for structural concrete applications. However, this research stands out by presenting three different types of aggregates, varying only in the percentage of residue used in each composition, and by producing aggregates with a shape similar to commercially available crushed stone used in construction. Another highlighted aspect of this study is the demonstration of the stages involved in refining the production process to provide better understanding for the reader.

In the initial phase, twenty-five sample types were produced, varying the amount of residue and sintering time. Based on specific characterization analyses, the process advanced to a second stage, called the first production cycle, in which four types of samples were tested with variations in both the residue percentage and sintering time. In the third stage, or second production cycle, the variation was solely in the percentage of residue used, while maintaining a constant sintering temperature of 1200°C.

A third stage, or third production cycle (the current phase), was necessary to adjust the geometric conformation of the three aggregate types and to correct the high porosity and void index observed in AGS90. This required an increase in the sintering temperature to 1250°C, resulting in a darker appearance compared to AGS70 and AGS80, which were produced at 1200°C and retained a more reddish color.

II. Material And Methods

For the production of synthetic coarse aggregate, three raw materials were used: kaolinitic clay, acquired from the ceramic industrial hub of São Miguel do Guamá-PA, extracted with authorization from the competent environmental agencies; silica (sand with low iron concentration), purchased from the civil construction market in Belém-PA; and bauxite residue (BR), supplied by the company Hydro-ALUNORTE in Barcarena-PA and stored in the Civil Engineering Laboratory at UFPA.

The clay, silica, and bauxite residue were dried in an oven with air recirculation at a temperature of 105°C for 24 hours to remove excess moisture and prevent crack formation in the aggregate. They were also disaggregated using a ball mill, model WORK INDEX series 005, followed by a disk mill for 30 minutes. These processes are necessary to achieve better granulometric control, using particles smaller than 150 µm. It is important to note that silica has a spherical morphology and a high surface area when the particle diameter is less than 150 µm, which increases the efficiency of sintering reactions¹⁴.

The research phases initially involved a primary process followed by three improvement processes corresponding to three production cycles. This study aims to indicate the technical feasibility of using these synthetic coarse aggregates in structural concrete.

Table no 1: Percentage of residue, temperature, and sintering time of aggregate samples – Preliminary stage.

Sample	Bauxite residue (%)	Temperature (°C)	Time (h)
C1	60	1250	3
C2	60	1250	3
C3	70	1250	3
C4	60	1250	3
C5	70	1250	3
C6	60	1250	3
C7	80	1250	3
C8	70	1250	3
C9	80	1200	2
C10	60	1250	3
C11	75	1250	3
C12	75	1250	0,5
C13	75	1200	3
C14	75	1250	3
C15	60	1225	3
C16	70	1250	3

C17	70	1200	3
C18	70	1250	3
C19	70	1225	3
C20	70	1200	3
C21	70	1150	3
C22	80	1200	3
C23	85	1150	3
C24	80	1150	3
C25	77,5	1150	3

After the preparation of the raw materials, the experimental process for producing twenty-five types of samples was initiated by mixing the raw materials—bauxite residue, silica, clay, charcoal as biomass, and lime—identified as C1 to C25, as shown in Table 1. These samples underwent treatment and homogenization in a ball mill for 30 minutes. After homogenization, they were placed in a dry rotary drum and a continuous extruder to form the aggregates into pellets. Subsequently, the pellets were dried in an oven at 105°C for 24 hours before proceeding to sintering at different temperatures and durations.

The synthetic aggregates sintered using the rotary drum method are shown in Figure 4, with diameters ranging between 0.5 and 1.5 cm.

Figure 1: Appearance of pelletized synthetic aggregates after sintering.

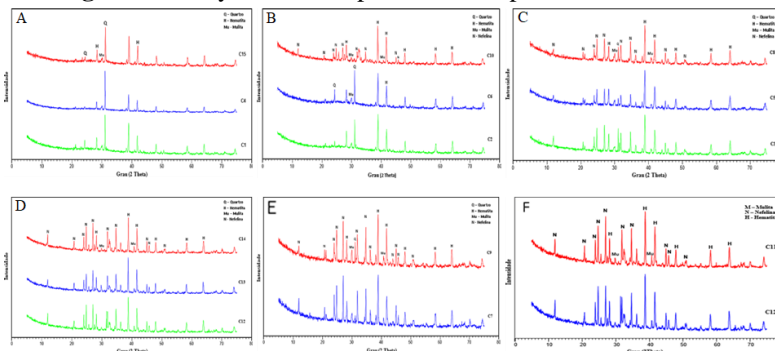


Figure 1 shows the completed sintering process, which represents the closing of pores associated with the mechanical strength of the aggregates. The efficiency of solid-state reactions is responsible for the formation of mullite and the vitreous phase. These interactions can be controlled through adjustments in the granulometry of raw materials, sintering temperature and time, and matrix formulation^{14,15}.

The samples underwent X-ray diffraction (XRD) analysis, and the results indicated the presence of quartz, hematite, mullite, and nepheline minerals. Mullite was found in all samples, identified through its characteristic peaks. The amount of mullite formed is associated with an increase in the mechanical strength of ceramic materials. Studies conducted by¹⁴ showed that the reduction in quartz content is related to the increased formation of mullite.

Figure 2 presents the XRD analyses of the samples containing 60% to 80% bauxite residue, corresponding to C1 to C15, sintered at temperatures ranging from 1225°C to 1250°C. The analyses at different sintering temperatures aimed to verify the influence of this variable on the formation of new mineral phases.

Figure 2: X-ray diffraction pattern of samples C1, C4, and C15.



In panel A of Figure 2, the diffraction pattern shows the presence of quartz, hematite, and mullite minerals. In sample C15, even at a lower sintering temperature compared to the other samples, the behavior of the crystalline phases is similar to C1 and C4, with no significant changes in the sample peaks. In panel B, sample C2 was influenced by biomass during the sintering process, sample C10 by lime, and sample C6 by silica in the mineralogical transformations. In sample C6, a more intense quartz peak is observed, indicating that part of the silica in the sample did not react to form new phases. Comparing the influence of lime and biomass in the composition, it is noted that lime had a greater impact on the formation of new phases, such as nepheline.

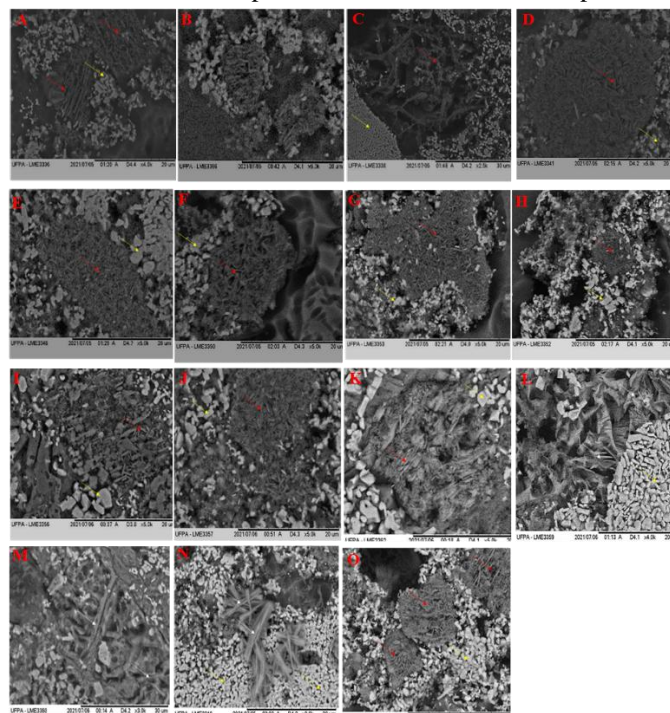
In this case, calcium and magnesium oxides present in the lime act as fluxes during sintering, forming a low-viscosity vitreous phase that facilitates the growth of crystalline phases. During the thermal treatment of bauxite residue, due to a considerable amount of sodium and silicon oxides, $\text{Na}_5\text{Al}_3\text{Si}_3\text{O}_{15}$ species—precursors of nepheline—are formed¹⁶. This can be confirmed by analyzing panels C to E, where the samples contain 70% or more bauxite residue in their composition, with nepheline as the predominant phase. The diffraction patterns of samples C3, C5, and C8, which contain 70% residue and were sintered at 1250°C, are shown in panel 3. These samples contain 25%, 15%, and 30% clay, respectively. It is also observed that there is a similarity in the formed phases among the samples, with some differences in the intensities of the quartz, hematite, mullite, and nepheline peaks.

In panel D, samples C12, C13, and C14, which have the same raw material composition but were sintered at different temperatures and durations (1250°C for 0.5 h, 1200°C for 3 h, and 1250°C for 3 h, respectively), are compared to evaluate the influence of these variables on mineral transformations. Based on the X-ray diffraction results, an increase in temperature led to a greater formation of nepheline, as indicated by the higher peak intensity in samples C12 and C14. Regarding the sintering time, no significant differences in peak intensity were observed between samples C12 and C14, suggesting the possibility of reducing the sintering duration. In panel 5, diffraction patterns of samples C7 and C9, which have the same raw material composition but were sintered at 1250°C for 3 hours and 1200°C for 2 hours, respectively, are analyzed. In sample C7, greater mullite formation was observed, leading to higher intensity in its characteristic peaks. In panel F, diffraction patterns of samples C11 (0.5 hours) and C12 (3 hours), which have the same raw material composition, were compared to assess the influence of sintering time on the formation of new phases. Based on the results, no significant changes were observed between the two samples, although the peaks related to the nepheline phase showed slight differences when comparing the two diffraction patterns. This suggests the possibility of reducing the sintering time while maintaining the mineralogical characteristics of the material.

Figure 3 presents the scanning electron microscopy (SEM) analyses for the aggregate samples from C1 to C15, according to the composition, temperature, and sintering time characteristics shown in Table 1.

The SEM analysis was necessary to observe the phase formations in the aggregate during sintering, such as the vitreous phase and mullite. Mullite is commonly found in ceramic minerals, typically in the form of flakes and needles. It originates from composite phases such as alumina and silica from kaolin, with the primary form appearing as flakes. Mullite that crystallizes from molten or low-viscosity phases, forming needle-like structures, is termed secondary mullite. When derived from kaolinite, it appears as needle-shaped structures at temperatures above 1200°C, depending on the level of impurities present or the assistance of molten phases¹⁴.

Figure 3: Scanning Electron Microscopy of Samples C1 to C15. a) C1 at 4000x magnification. b) C2 at 5000x. c) C3 at 2500x. d) C4 at 5000x. e) C5 at 5000x. f) C6 at 5000x. g) C7 at 5000x. h) C8 at 5000x. i) C9 at 5000x. j) C10 at 5000x. k) C11 at 5000x. l) C12 at 4000x. m) C13 at 3000x. n) C14 at 3000x. o) C15 at 5000x. White arrow: unidentified phase; Yellow arrow: vitreous phase.



The preliminary results of scanning electron microscopy indicate the presence of secondary mullite with an acicular morphology. This formation occurs in post-reactive processes through solid-state reactions or thermal decomposition. In the case of stoichiometric mixtures of alumina and silica powders, mullite formation occurs between temperatures of 1400 and 1800°C. However, when dealing with bauxite residue, this temperature can be reduced due to the presence of fluxing oxides, which form a low-viscosity vitreous phase, facilitating the growth and formation of secondary mullite crystals.

After the initial experimental stage, the subsequent stages were referred to as production cycles. In the first cycle, four types of synthetic coarse aggregates were produced, followed by three in the second cycle, and finally, three more in the third cycle. These were developed by the engineering team at the Chemistry Laboratory of the Federal University of Pará. The samples were identified in the first cycle as A1, A2, A3, and A4, while in the second and third cycles, they were labeled AGS70, AGS80, and AGS90, corresponding to compositions containing 70%, 80%, and 90% bauxite residue, respectively.

Figure 4 illustrates the progress in improving the conformation (physical aspects) of these aggregates up to the current phase (third cycle). Table 1 presents the characterization tests conducted, following the NBR 7211:2022¹⁷ standard, carried out in the Civil Engineering Laboratory of the Federal University.

Figure 4: Samples from the first stage of the AGS production process. Samples designated as A1, A2, A3, and A4.

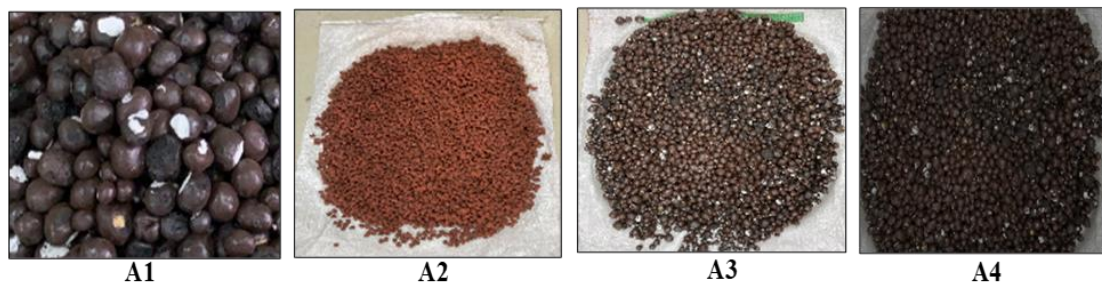


Figure 7 shows photographs of the samples in rounded shapes with the following designations: A1, containing 60% bauxite residue in its composition; A2, with 85%; A3, with 85%; and A4, with 80%. Leaching and solubilization tests were also conducted, indicating the feasibility of producing synthetic aggregates at this stage, even with concentrations above 80%, while maintaining safety standards—particularly regarding NaOH content, which remains within the limits required by leaching and solubilization regulations. In this context, samples A2 to A4 contained the highest amounts of bauxite residue, increasing its reuse without compromising physical characteristics or application potential, as presented in Table 2.

Table no 2: Composition, temperature, and sintering time of aggregate samples – First production cycle.

Sample	Bauxite Residue (%)	Sílica (%)	Clay (%)	Lime (%)	Temperature (°C)	Time (h)
A1	60	15	25	-	1250	3
A2	85	10	5	-	1150	3
A3	85	10	5	-	1200	3
A4	80	15	5	-	1200	3

In order to increase the consumption of bauxite residue and the scale of aggregate production, some adjustments were made to the process aiming for a production of 350 kg/week of aggregate. The adjustments resulted in three types of aggregates (AGS70, AGS80, and AGS90), as shown in Table 3.

Table no 3: Composition, bulk density, temperature, and sintering time of the aggregate samples.

Sample	Bauxite Residue (%)	Sílica (%)	Clay (%)	specific gravity (g/cm ³)	Temperature (°C)	Time (h)
AGS70	75 - 70	20 - 25	5	< 1,5	1200	3
AGS80	85 - 80	10 - 15	5	> 1,5 e < 2,0	1200	3
AGS90	95 - 90	0 - 5	5	> 2,0	1200	3

The aggregate samples presented in Table 3 are based on the results obtained so far, which indicated that it would be possible to produce synthetic aggregates in different proportions of raw materials (bauxite residue, silica, and clay) and, primarily, in line with the specifications of commercially used aggregates (light, normal, and heavy). Additionally, the use of the AGS70, AGS80, and AGS90 samples aims to increase the production scale of the aggregate and consequently the consumption of bauxite residue.

In the production of the AGS70, AGS80, and AGS90 samples, control was carried out through the composition ranges, bulk density, temperature, and sintering time to ensure compliance with legislation for

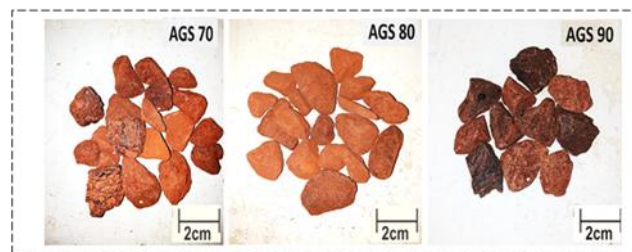
potential commercialization of the product. The bulk density values were controlled to produce aggregates similar to those used commercially. Figure 5 shows the physical aspects of the synthetic coarse aggregates in the second stage of production.

Figure 5: Samples from the second stage of the AGS production process. Samples designated AGS70, AGS80, and AGS90.



At this stage of the research, AGS70 had a maximum diameter of 19.0 mm, a fineness modulus of 7.37, a shape index of 1.39, an abrasion loss (Los Angeles) of 31.0%, and a water absorption of 2.60%. AGS80 had a maximum diameter of 19.0 mm, a fineness modulus of 6.71, a shape index of 1.77, an abrasion loss (Los Angeles) of 38.0%, and a water absorption of 8.12%. AGS90 had a maximum diameter of 19.0 mm, a fineness modulus of 6.55, a shape index of 1.61, an abrasion loss (Los Angeles) of 42.2%, and a water absorption of 11.35%.

Figure 6: Samples from the second stage of the AGS production process. Samples designated AGS70, AGS80, and AGS90



With the aim of maintaining the consumption of bauxite residue and the production scale of the aggregates as outlined in the previous stage, but making some adjustments to the process primarily aimed at reducing the porosity of AGS90 and adapting the shape of the aggregates to a more lamellar and even cylindrical appearance (Figure 7), these adjustments led to changes in the specific mass of these aggregates and an increase in the sintering temperature of AGS90, as shown in Table 4.

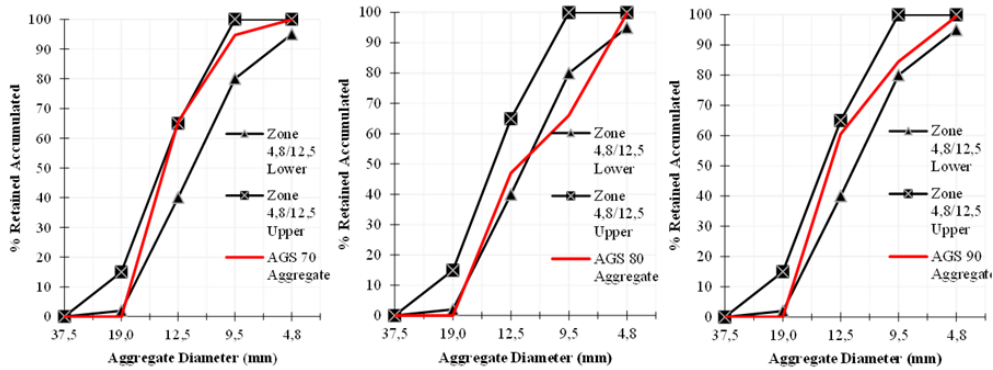
Table no 4: Composition, bulk density, temperature, and sintering time of the aggregate samples.

Sample	Bauxite Residue (%)	Sílica (%)	Clay (%)	specific gravity (g/cm ³)	Temperature (°C)	Time (h)
AGS-70	75 - 70	20 - 25	5	2,21	1200	3
AGS-80	85 - 80	10 - 15	5	2,26	1200	3
AGS-90	95 - 90	0 - 5	5	2,41	1250	3

At this stage of the research (current), as shown in Figure 9, AGS70 has a maximum diameter of 19.0 mm, a fineness modulus of 1.95, a shape index of 2.07, an abrasion loss (Los Angeles) of 41.06%, and a water absorption of 6.50%. AGS80 has a maximum diameter of 19.0 mm, a fineness modulus of 1.66, a shape index of 2.08, an abrasion loss (Los Angeles) of 43.94%, and a water absorption of 5.24%. AGS90 has a maximum diameter of 19.0 mm, a fineness modulus of 1.84, a shape index of 1.99, an abrasion loss (Los Angeles) of 27.41%, and a water absorption of 3.20%.

Table 5 summarizes the characterization tests performed, as per the standard (NBR 7211, 2022)¹⁷, conducted at the Civil Construction Materials Laboratory (LeMaC) and the Concrete Laboratory (LaCon) of the Civil Construction Laboratory at the Federal University of Pará. A total of 100 kg of each sample was used, as established by (NM 26, 2009)¹⁸. Aliquots of the samples were sieved dry to comply with the standard (NBR 7211, 2022)¹⁷, with sizes ranging from crushed 0 (4.75 mm to 12.5 mm) and 1 (9.50 mm, restricted to 19.0 mm).

Figure 7: Granulometric distribution of the samples from the second and third production cycles, respectively: (A/D) AGS70; (B/E) AGS80; and (C/F) AGS90.



Regarding the particle sizes, these aggregates are classified as coarse aggregates according to (NBR 7211, 2022) [1]. According to (Souza, 2010)¹⁴, there is no ideal granulometry for a given aggregate, as the general goal is to achieve a balance between physical and economic requirements. A balanced granulometric distribution will result in more workable and economical concrete mixes, as well as a more compacted concrete mass, reducing the volume of voids and, consequently, the spaces through which potentially aggressive agents could penetrate the concrete. Among the other studies used as the basis for this work, only ^{19,20} presented results regarding the granulometric distribution of bauxite residue. However, it is important to highlight that there is still a significant gap in information on this subject, as shown by the results obtained by²¹.

III. Result And Discussion

The synthetic coarse aggregates were produced and made available by the Chemical Engineering Laboratory to the Civil Engineering Laboratory at the Federal University of Pará. The produced aggregates were sent without any separation by diameter for better classification into granulometric ranges, and an estimated percentage of 1% of the total sent showed some production defects, as shown in Figure 9. After removing the aggregates with defects, it was decided to restrict the study in this research to aggregates with dimensions retained on the #4.8mm sieve and passing through the #19.0mm sieve.

Figure 8: Example of nonconformity in the AGS90 sample.



The granulometric distribution of the samples from the second and third production cycles after adjustments in the granulometric ranges of the synthetic coarse aggregates, according to the (NBR 7211, 2022) standard, is shown in Figure 8. The results obtained from the granulometric curves showed that in the third cycle (the current stage of the research), AGS70 and AGS90 were entirely within the #4.8-19.0mm granulometric range, while AGS80 did not have enough particles to fit into the granulometric range between the #6.3-9.5mm sieves. However, all three types studied exhibited well-distributed granulometric curves, making them suitable for use in the production of Portland cement concrete.

Figure 9: Average specific masses of the tested samples.

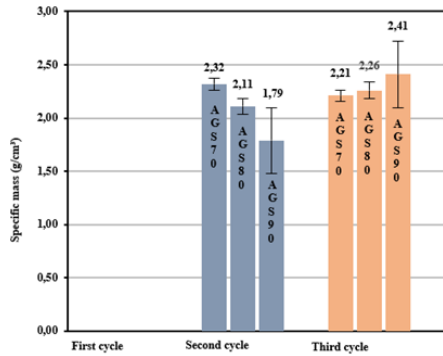
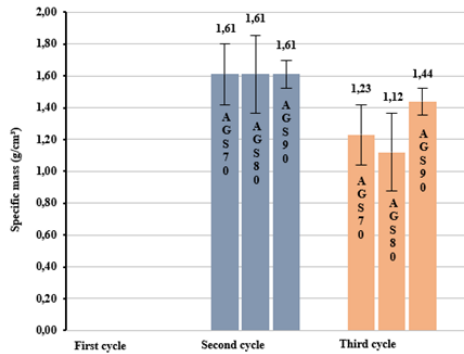


Figure 10: Average unit mass of the tested samples.



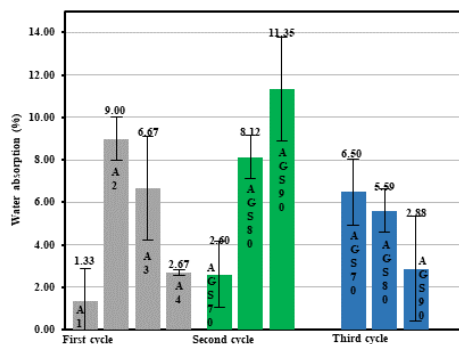
The specific mass of aggregates derived from rocks, commonly used in construction, ranges from 2.60 g/cm³ to 2.70 g/cm³, while the unit mass of normal aggregates ranges from 1.38 g/cm³ to 1.58 g/cm³. The research took these assumptions into consideration for evaluating the results. However, in the first production cycle, specific and unit masses were not evaluated²⁴. In the second cycle, information about the aggregate masses can be observed, but due to the unsatisfactory shape of the aggregates (Figure 6), it was necessary to produce a third cycle (the current shape). Figures 10 and 11 illustrate the results obtained in the third cycle, where the specific mass varied from 2.21 g/cm³ to 2.41 g/cm³, and the unit mass varied from 1.23 g/cm³ to 1.44 g/cm³.

To be classified as lightweight, aggregates must have an apparent specific mass (MEA) value lower than 2 g/cm³. European standards, on the other hand, state that lightweight aggregates, intended for use in concrete and mortar, must have a unit mass lower than 1.20 g/cm³ and a specific mass not exceeding 2.0 g/cm³²³. They further assert that lightweight aggregates are typically those with a unit mass lower than 1.2 g/cm³, with this low density directly related to their cellular or highly porous microstructure²⁴.

In this research, the aggregates from the second and third cycles, due to their specific masses being higher than 2.0 g/cm³, are classified as traditional aggregates.

It is important to emphasize that, as with most of the studies used as the foundation for this research, the sample production occurred at firing temperatures above 1200°C, and muffled furnaces were used for the production of AGS. Rotating furnaces would be the most suitable for ensuring proper and homogeneous temperature distribution, thus optimizing the production process while reducing energy expenditure.

Figure 11: Average results of the water absorption tests.



Some authors explain that the water absorption capacity of aggregates and the speed at which this phenomenon occurs depend on factors such as total porosity, pore connectivity, aggregate surface characteristics, and the moisture content of the aggregate before mixing²². Commercial aggregates typically exhibit water absorption, after 24 hours of immersion, of less than 20%²⁵. According to some authors, the morphology of the aggregate plays a significant role in controlling water absorption because when an aggregate has a more interconnected pore structure, it will absorb more water compared to a material with isolated pores and a vitreous surface²⁵. Another issue raised by these authors concerns the firing temperature, which plays a fundamental role in controlling the water absorption capacity. This is because the sintering of the mixture promotes particle densification, reducing the ingress of water into the aggregate matrix.

The high porosity index of the aggregate is directly related to its water absorption capacity. The higher the percentage of porosity in the material, the greater its water absorption capacity. Two adverse conditions are highlighted in relation to the high percentage of water absorption in aggregates in concrete. The first is negative, as excessively porous aggregates are directly detrimental to hardened concrete, causing issues such as shrinkage due to drying, increased specific mass, and reduced fire resistance¹⁹. The second is positive, bringing benefits such as improving the properties of the transition zone between the aggregate and the cement paste, reducing the wall effect, and enhancing internal curing.

Figure 12 shows the average results of the water absorption tests for the three production cycles through the improvement process, both in terms of sample conformation and the reduction of porosity. It is noted that the samples tested in the third cycle exhibited absorption rates between 2.88% and 6.50%. Therefore, at this stage, the aggregates already met the limits established by the (NBR 7211, 2022)¹⁷ standard. However, they still did not correspond to aggregates produced from rocks, which typically have water absorption between 1% and 2%. The water absorption properties of aggregates directly influence the conditions of the concrete in its fresh state, as well as the cement hydration process.

Figure 12: Average results of the amount of fine material passing through the 75 µm sieve by washing.

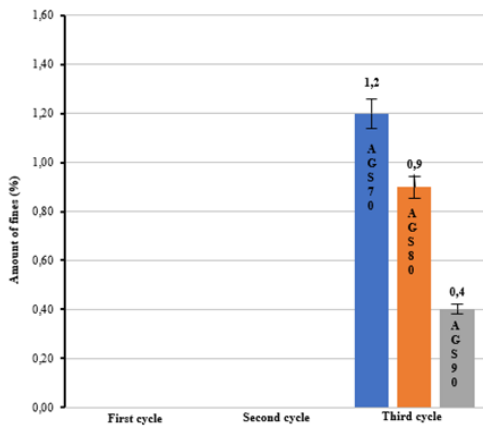
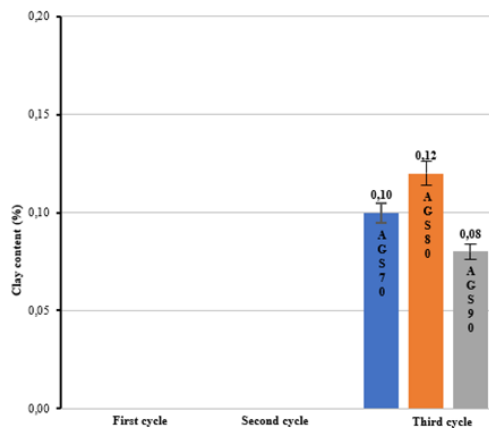


Figure 13: Average results of clay lumps and friable materials present in the samples.



Clay lumps and friable materials alter the granulometric characteristics of coarse aggregates and reduce the strength of both the aggregate itself and the concrete made with it²². Aggregates that have high levels of clay lumps and friable materials can cause modifications in the appearance of the concrete, potentially leading to stains on its surface. The percentage of clay lumps and friable materials in aggregates should not exceed 3.0%¹⁷. Only in the third production cycle were the percentage of fine material (Figure 14) and the presence of clay lumps and friable materials (Figure 15) evaluated. The analysis showed that all the tested samples passed, as the values obtained for fine material ranged from 0.4% to 1.20%, and for friable materials and clay lumps, they ranged from 0.08% to 0.12%.

Figure 14: Results of the shape index tests of coarse aggregates using the caliper method.

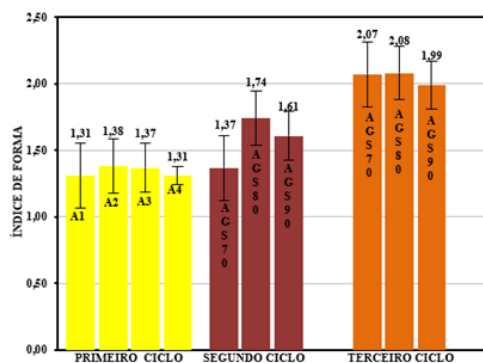
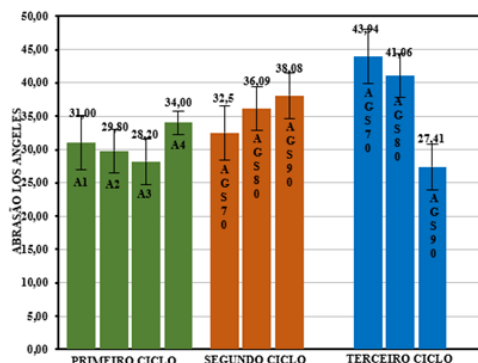
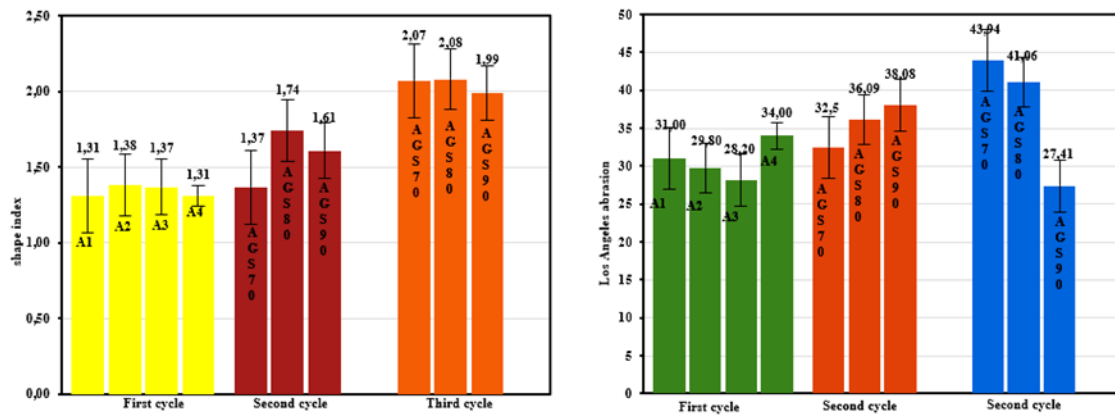


Figure 15: Average results of Los Angeles abrasion wear indices.





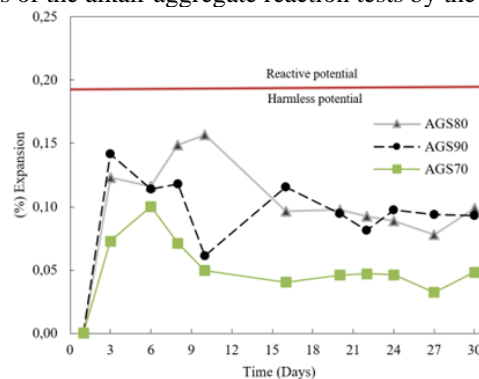
According to Borba and Santos (2019)²⁶, the shape index of coarse aggregate grains indicates how closely they resemble a cube. Such a shape ensures the interlocking of the coarse aggregate when compacted, thus increasing its shear strength. However, the NBR 7211, 2022¹⁷ states that the shape index of a coarse aggregate, determined in accordance with NBR 7809, 2016²⁷, must not exceed 3, allowing for aggregates with a lamellar shape. Figure 14 presents the average shape indices found for the tested samples. For the current stage of the research, the result to be considered is from the third cycle, where it is possible to observe that all samples remained below the regulatory limit, thus meeting the required standards.

Following the same criteria previously used to analyze the shape index, and observing the results obtained in the third production cycle regarding water absorption (Figure 11), it is important to note that highly porous aggregates are typically more fragile, making them unsuitable for structural concrete production. However, Figure 15 presents the average results of the Los Angeles abrasion index, conducted according to the NM 51, 2001²⁸ standard, where the analyzed samples showed abrasion resistance between 27% and 43.94%. These indices are considered satisfactory since the NBR 7211, 2022¹⁷ stipulates that the mass loss percentage should be less than 50%.

It is worth noting that the higher the water absorption of the aggregates, the greater the mass loss through the abrasion test. Furthermore, the results obtained in this research demonstrated that the coarse aggregates are suitable for use in the production of concrete for various purposes, as abrasivity is directly related to axial compression and durability. In this case, the samples tested showed superior performance compared to riverbed pebbles, which are commonly used aggregates in the North of the country, as these typically have higher abrasion loss values around 50%.

Durability tests were conducted to qualitatively assess the condition of the aggregates, through alkali-aggregate reaction tests, sulfate resistance tests, and X-ray diffraction, with the primary aim of ensuring that the third-cycle aggregates do not contain conditions that would limit their use in Portland cement production.

Figure 16: Results of the alkali-aggregate reaction tests by the accelerated method.



The tests were conducted according to the criteria established by (NBR15577-4, 2018)²⁹, and the chosen cement was type CP IV due to the high amount of pozzolana included in the composition. The graph in Figure 16 shows the behavior of the mortar expansion over a 30-day period, and the results qualitatively indicated that synthetic aggregates produced from bauxite residue at various levels, under the conditions stated in the third cycle, do not exhibit reactivity potential with the alkalis in the studied cement, meaning they are inert.

Figure 17: Durability evaluation tests of the AGS90 from the third production cycle. A) Initial dry sample retained on sieves #19.0mm and #12.5mm. B) Detail of the sample immersed in NaSO4 solution (a,b), appearance after undergoing the fifth cycle (c), and C) final dry sample, fragmented and retained on sieves #19.0mm to #4.8mm.



Figure 18: Durability test results of the aggregate according to DNIT 446/2024-ME.

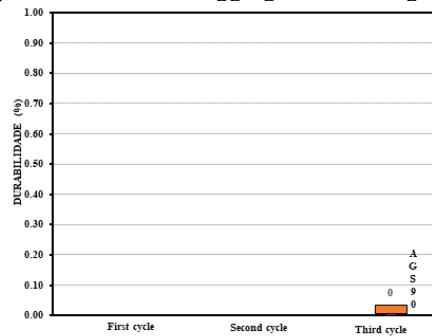
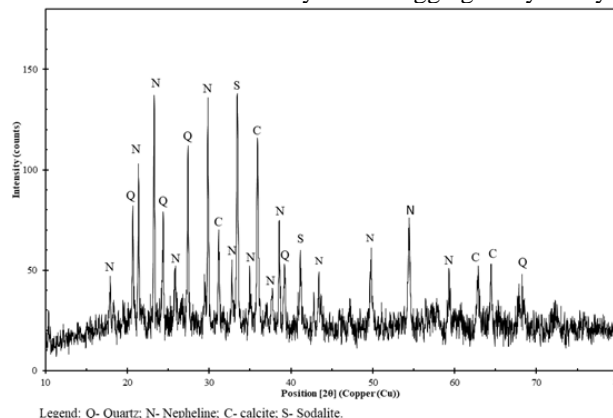


Figure 18 A summary of the washing stages of the aggregates using sodium sulfate and barium chloride solutions for the AGS90 from the third production cycle, following a process divided into five cycles as recommended by (DNIT 446/2024-ME)³⁰ to determine the resistance of the aggregates over time. The AGS90 was chosen to represent the third-cycle aggregates due to its higher percentage of residue in its composition.

The maximum permissible limits for the results of this durability test, according to (DNER 037/1997-ME)³¹, should not show a loss greater than 12%. The tested sample showed no disintegration when exposed to these sulfates, with a durability index for disintegration of 0.00%, as shown in Figure 19.

Additionally, an important analysis was performed using X-ray diffraction on the AGS90 from the third production cycle to identify the mineral phases in this sample. The result obtained is presented in Figure 20 and will be analyzed subsequently.

Figure 19: Mineral Identification of AGS90 Synthetic Aggregate by X-ray Diffraction (XRD).



Based on the X-ray diffraction (XRD) results, the main peaks identified are Nepheline (Na,K)AlSiO₄ or feldspar, Sodalite (Na₄Al₃(SiO₄)₃Cl), Calcite (CaCO₃), followed by peaks of Quartz (SiO₂), which indicate a stable condition for the produced sample. Additionally, through the lower intensity peaks, the presence of minerals such as iron and zeolite was also observed. This graphical configuration suggests that a significant amount of amorphous material is present, and its mineral phases represent an inert compound. This is a highly satisfactory condition for a synthetic coarse aggregate.

To validate the chemical characterization of the synthetic coarse aggregate, Table 6 presents the results obtained through X-ray fluorescence analysis for the main oxides.

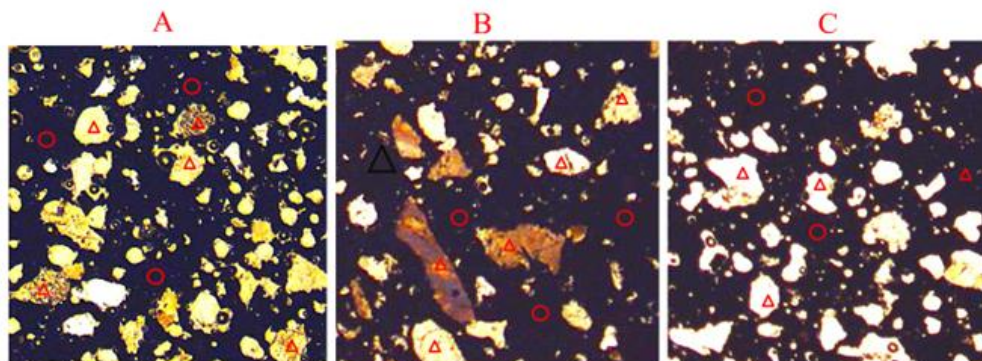
Table no 6: Test FRX

Compound	Concentration m/m (%)
SiO ₂	28,74
TiO ₂	5,42
Al ₂ O ₃	21,29
Fe ₂ O ₃	31,7
MnO	0,14
MgO	0,12
CaO	1,23
Na ₂ O	9,08
K ₂ O	0,14
P ₂ O ₅	0,11
SO ₃	0,28
LOI	0,99

Based on the results obtained from the X-Ray Fluorescence test, there was a predominance of silicon oxides (SiO₂) at 28.74%, followed by aluminum oxides (Al₂O₃) at 21.29%, sodium oxides (Na₂O) at 9.08%, and titanium oxides (TiO₂) at 5.42%. It is also important to highlight the presence of elements such as potassium oxide (K₂O), manganese oxide (MnO), and magnesium oxide (MgO), which could contribute to the product being considered expansive.

According to the XRD results, the main identified peaks are for Calcite (CaCO₃), followed by peaks for quartz (SiO₂), ensuring a stable condition for the produced sample. Furthermore, it is necessary to note that through peaks of lower intensities, the presence of the following minerals was also identified: iron and zeolite. Thus, this graphical configuration indicates the presence of a large amount of amorphous material, and its mineral phases are represented as an inert compound. This condition is very satisfactory for a synthetic coarse aggregate.

Figure 20: Images through optical microscope of the third production cycle samples (A/B/C - AGS 70/80/90 respectively) under polarized light.



Caption: ○ Presence of Bauxite; △ Residue

In the images obtained through an optical microscope using polarized light, as shown in Figure 20, the distribution of the constituent materials of the synthetic coarse aggregates from the third production cycle is highlighted. The dark areas in the images represent the occupation of the residue, and the other particles are sections of silica sand and clay particles. It is also possible to observe in the images of frame C that the greater the use of bauxite residue, the lower the densification of silica in the sample, which presents a challenge, as silica directly contributes to the vitrification of the material, ensuring a reduction in porosity and an increase in mechanical strength and modulus of elasticity. However, as a compensating criterion, AGS90 was sintered at a temperature of 1250 °C, resulting in a 50 °C difference compared to AGS70 and AGS80 for increased vitrification of the material

IV. Conclusion

This study aimed to explore the production of synthetic coarse aggregates (AGS) using bauxite residue from the Hydro mining company in Barcarena-PA. The process was optimized in three stages, focusing on the geometric shape, specific mass, mechanical strength, and durability of the aggregates. In the final stage, aggregates were produced with residue percentages between 70% and 95%, at temperatures ranging from 1200°C to 1250°C.

Physical and mechanical tests confirmed that the aggregates from the second cycle met most normative parameters (NBR 7211, 2022), with the exception of AGS90's water absorption, which exceeded 10%, making it unsuitable for structural concrete. To improve these properties, a third cycle was conducted, resulting in improved geometric conformation and better performance, particularly in Los Angeles abrasion.

Durability tests, including sodium sulfate and barium chloride solutions and alkali-aggregate reaction (AAR) tests, confirmed that the bauxite residue does not present a reactive potential to cement alkalis, indicating its suitability for use in foundation concrete. The third-cycle aggregates fully met the relevant standards and showed the best results in abrasion, shape index, and water absorption.

In conclusion, this research demonstrates the environmental benefits of using in natura bauxite residue for producing synthetic coarse aggregates, reducing reliance on natural resources like river pebbles and mitigating the environmental impacts of extraction, transport, and CO₂ emissions.

Acknowledgments

The authors would like to thank HYDRO, the Brazilian funding agency CAPES, and PPGEC for the master's and doctoral scholarships, which were essential for the completion of this study. Additionally, we express our gratitude to LEC and LEQ (Civil Engineering and Chemistry Laboratories of the Federal University of Pará), the CPRM analysis laboratory, and UNIFESP for allowing some of the analyses conducted in this research.

References

- [1]. Oliveira, Drcde, Rossi, CRC. Concretes With Red Mud Coarse Aggregates. *Materials Research*, V. 15, N. 3, P. 333–340, Maio 2012.
- [2]. Albuquerque, NG. Estudo Das Propriedades Mecânicas De Concretos Dosados Com Agregados Produzidos A Partir De Lama Vermelha. Trabalho De Conclusão De Curso (Graduação). UFPA - Departamento De Engenharia Civil, 2007.
- [3]. ALCOA (2024). <https://www.alcoa.com/brasil/pt>.
- [4]. Araújo, ER, Olivieri, RD & Fernandes, FRC. Atividade Mineradora Gera Riqueza E Impactos Negativos Nas Comunidades E No Meio Ambiente. 2014.
- [5]. Bertocchi, AF, Ghiani, M., Peretti, R. & Zucca, A., (2006). Red Mud And Fly Ash For Remediation Of Mine Sites Contaminated With As, Cd, Cu, Pb And Zn. *Journal Of Hazardous Materials*. 134, 112-119, 2006
- [6]. Associação Brasileira De Normas Técnicas, NBR 10004-1 (2024). Resíduos Sólidos – Classificação.
- [7]. Ribeiro, DV & Morelli, MR. Estudo Da Viabilidade Da Utilização Do Resíduo De Bauxita Como Adição Ao Cimento Portland. In: Congresso Brasileiro De Engenharia E Ciência Dos Materiais, Pernambuco, 2008.
- [8]. Venâncio, L. C. A., (2013). Desenvolvimento De Unidade Piloto De Transferência De Massa Gás/Líquido: Redução Da Reatividade Do Resíduo Da Indústria De Alumina Através De Reação Com Gases De Combustão. (Tese De Doutorado). Universidade Federal Do Pará, Belém, PA, Brasil.
- [9]. Rosário, KA. Concreto Com Utilização De Agregado Graúdo Sintético Produzido A Partir Da Lama Vermelha: Estudos De Dosagem, Propriedades E Microestrutura. (Dissertação De Mestrado). Universidade Federal Do Pará, Belém, PA, Brasil, 2013.
- [10]. Tsakiridis, PE, Agatzini-Leonardou, S., Oustadakis, P. Red Mud Addition In The Raw Meal For The Production Of Portland Cement Clinker. *Journal Of Hazardous Materials*. 103-110, 2004.
- [11]. Guo, T., Yang, H., Liu, Q., Hannian, G., Wang, N., Yu, W., & Dai, Y. (2018). Adsorptive Removal Of Phosphate From Aqueous Solutions Using Different Types Of Red Mud. *Water Sci. Technol.* 2017, 570-577, 2018.
- [12]. Santos, DH. Influência Da Sílica E Temperatura Nas Propriedades Físicas Dos Agregados Sintéticos Produzidos Com Resíduo Do Processo Bayer. (Tese De Doutorado). Universidade Federal Do Pará, Belém, PA, Brasil, 2019.
- [13]. Cunha, MVPO & Corrêa, JAM. Síntese E Caracterização De Hidróxidos Duplos A Partir Da Lama Vermelha (Synthesis And Characterization Of Layered Double Hydroxides From Red Mud). *Revista Cerâmica*, 57, 85- 93, 2011.
- [14]. Souza, J. Estudo E Avaliação Do Uso De Resíduos Do Processo Bayer Como Matéria Prima Na Produção De Agregados Sintéticos Para A Construção Civil. (Tese De Doutorado). Universidade Federal Do Pará, Belém, PA, Brasil, 2010.
- [15]. Mörtel, H., Heimstadt, K. Mikrobielle Werkstoffzerstörung - Simulation, Schadensfälle Und Gegenmaßnahmen Für Anorganische Nichtmetallische Werkstoffe: Keramik. *Materials And Corrosion*, 45(2), Pp. 128-136, 1994.
- [16]. Viegas, B. M., Et Al. A Influência Da Temperatura Nas Transformações De Fases Dos Minerais Presentes Na Lama Vermelha: Redução Da Hematita À Magnetita. *Matéria (Rio De Janeiro)*, V. 25, 2020.
- [17]. Associação Brasileira De Normas Técnicas, NBR 7211 (2022). Agregados Para Concreto – Requisitos.
- [18]. Associação Brasileira De Normas Técnicas, NBR NM 26 (2009): Agregados: Amostragem.
- [19]. Rossignolo, J. A., (2009). Concreto Leve Estrutural: Produção, Propriedades, Microestrutura E Aplicações. Pini.
- [20]. Reis, A. W. (2014). Caracterização Mineralógica Do Agregado Obtido A Partir Da Lama Vermelha Do Processo Bayer. (Dissertação De Mestrado). Universidade Federal Do Pará, Belém, PA, Brasil.
- [21]. Souza, P. H. R., Arraes, L. A. X., Marques, M. S. P., & Santos, J. C. M., (2019). Utilização Da Lama Vermelha Para A Produção De Agregado Sintético. *Revista Científica Multidisciplinar Núcleo Do Conhecimento*, 6(3), 30-43.
- [22]. Mehta PK, Monteiro PJM. *Concreto: Microestruturas, Propriedades E Materiais*. 2. Ed. São Paulo: Nicole Pagan Hasparyk; 2014.
- [23]. Associação Brasileira De Normas Técnicas, NBR 12655 (2022). Concreto De Cimento Portland – Preparo, Controle, Recebimento E Aceitação – Procedimento.

- [24]. Santos, D. H., Dalmeida, A. P., Figueiredo, W. B., Valente, A. L., & Souza, J. A. S., (2014). Utilização Do Rejeito Do Processo De Bayer Como Matéria Prima Na Produção De Agregados Leves. In: XX Congresso Brasileiro De Engenharia Química, Florianópolis, SC, Brasil.
- [25]. Tuan, B. L. A., Hwang, C. L., Lin, K. L., Chen, Y. Y., & Young, M. P., (2013). Development Of Lightweight Aggregate From Sewage Sludge And Waste Glass Powder For Concrete. *Construction And Building Materials*, 47, 334-339.
- [26]. Borba VQ, Santos AA. Projeto De Base Drenante Realizado De Acordo Com A Especificação Técnica DER/SP ET-DEP00/008 [Trabalho De Conclusão De Curso]. Criciúma: Universidade Do Extremo Sul Catarinense; 2013.
- [27]. Associação Brasileira De Normas Técnicas. NBR 7809 (2019). Agregados Graúdo. Determinação Do Índice De Forma Pelo Método Do Paquímetro: Método De Ensaio.
- [28]. Associação Brasileira De Normas Técnicas. NBR NM 51 (2006). Agregado Graúdo: Ensaio De Abrasão “Los Angeles”.
- [29]. Associação Brasileira De Normas Técnicas. NBR 15577-4 (2018). Agregados: Ensaio De Reação Álcali- Agregado.
- [30]. Departamento Nacional De Infraestrutura Terrestre. DNIT 446/2024-ME: Agregado - Avaliação Da Durabilidade Pelo Emprego De Soluções De Sulfato De Sódio Ou Magnésio - Método De Ensaio.
- [31]. Departamento Nacional De Estradas E Rodagem. DNER 037/1997-ME: Agregado Graúdo Para Concreto De Cimento.